Influence of deformation-induced misalignment on the performance of hydrodynamic bearings: a comparison between rigid and flexible journal results

Xiaodong Sun
School of Engineering and Design, Technical University of Munich, Munich, Germany

Yuanyuan Liu
School of Electrical Engineering, Anhui University, Hefei, China, and

Bettina Chocholaty and Steffen Marburg
School of Engineering and Design, Technical University of Munich, Munich, Germany

Abstract

Purpose – Prior investigations concerning misalignment resulting from journal deformation typically relied on predefined misaligned angles. Nevertheless, scant attention has been devoted to the determination of these misaligned angles. Furthermore, existing studies commonly treat the journal as rigid under such circumstances. Therefore, the present study aims to introduce a framework for determining misaligned angles and to compare outcomes between rigid and flexible journal configurations.

Design/methodology/approach – The bearing forces are considered as an external load leading to journal deformation. This deformation is calculated using the finite element method. The pressure distribution producing the bearing force is solved using the finite difference method. The mesh grids in the finite element and finite difference methods are matched for coupling calculation. By iteration, the pressure distribution of the lubricant film at the equilibrium position is determined.

Findings – Results show that the deformation-induced misalignment has a significant influence on the performance of the bearing when the journal flexibility is taken into account. The parametric study reveals that the misalignment relies on system parameters such as bearing length-diameter ratio and static load.

Originality/value – The investigation of this work provides a quantification method of misalignment of hydrodynamic bearings considering the elastic deformation of the journal, which assists in the design of bearing in a rotor-bearing system.

Peer review – The peer review history for this article is available at: https://publons.com/publon/10.1108/ILT-10-2023-0337/

Keywords Hydrodynamic bearing, Misalignment, Flexibility, Journal deformation

Paper type Research paper

1. Introduction

Hydrodynamic bearings (HDB) are widely used in many mechanical devices, such as the connection pair of engine or stern propulsion systems of large marine ships. Due to journal flexibility, wear or inappropriate installation, misalignment inevitably occurs in an HDB-rotor system (Buckholz and Lin, 1986; Ram and C. Sharma, 2014; Jang and Khonsari, 2015). The misalignment between the journal and bearing bush can influence the dynamic behavior of the rotating system and the lubrication performance of the bearing (Bouyer and Fillon, 2002; Some and Guha, 2020). Therefore, it is critical to evaluate the influence of the misalignment.

The influence of misalignment on the performance of HDB has been extensively investigated. For instance, Sun and Gui (2004) studied the lubrication performances of a journal bearing considering the misalignment caused by journal deformation. Results show that the misalignment has an evident influence on the maximum pressure and the least thickness of the oil film.

Considering the interaction between rotation speed and misalignment angles, Huang and Yan (2020) analyzed the lubricant performance of a stern bearing. According to their study, the lubricant performance is closely related to the misalignment angle. Meanwhile, the misalignment angle is influenced by the rotation speed and loading capacity. Furthermore, by a dynamic response analysis, Lahmar *et al.*, 2002 found that the minimum film thickness and journal center trajectories are affected by misalignment, while the stability of the finite length bearing is also influenced (Abdou and Saber, 2020).

In recent years, the investigations on turbulent and thermal effects on the performance of aligned bearings have extended to the study of misalignment evaluation. Here, it is shown that a change in the flow regime from laminar to turbulent, together with an increase in misalignment angles, improved the load capacity of the bearing (Mallya *et al.*, 2017). Related to this study, Dick *et al.* (2004) found that increased bearing load and misalignment leads to higher peak bearing surface temperature. This effect is due to the rising viscous heat generation in the pressurized zone as a result of thinner film thickness. Abass and Kadhim (2013) found that there exists an interactive influence between surface roughness, thermal, journal misalignment and non-Newtonian behavior of lubricant effects on the thermohydrodynamic performance of the bearing. The work of Xu *et al.* (2015) indicated that the thermal effects have a significant effect on the lubrication of misaligned journal bearings under a large eccentricity ratio. The turbulence will obviously affect the lubrication of misaligned journal bearings when the eccentricity or misalignment ratio is large. Later, Guo *et al.* (2022) studied the mixed lubrication performance of a misaligned journal bearing considering the thermal effect. The experimental results show that visible wear appears at the end of the bush.

From the above-mentioned studies, the available research on the misalignment effect has obtained plenty of achievements. A common sense is that the misalignment effect has a significant influence on the performance of bearings. The commonly applied method introduces two misaligned angles into the conventional expression of the oil-film thickness (Sun and Gui, 2004; Xiang *et al.*, 2019; Zhang *et al.*, 2016; Dal and Karaçay, 2017; Zheng *et al.*, 2022; Yang *et al.*, 2023). The influence on the performance varies with the misaligned angles. On the one hand, however, the determination of the misaligned angles in a rotor-bearing system received little attention. In addition, some discussed misaligned angles are beyond the realistic ones, which leads to a loss of meaning related to engineering guidance. On the other hand, the journal is usually assumed to be rigid so that the journal inclination can be simply described by using two misaligned angles. In this way, the center line of the journal is considered straight, and the flexibility of the journal is ignored. In reality, however, the center line of the journal is bent due to the deformation caused by external loads (Ouyang *et al.*, 2023). The misalignment eccentricities and angles in different sections vary accordingly due to the existence of the bending deformation (He *et al.*, 2014). In this manner, the thickness and pressure of the lubricant film are affected such that the deformation-based misalignment influences the performance of the bearing. In addition, the bearing force contributes to the journal deformation. Therefore, there is an interaction between the bearing force and bending deformation. However, this interaction has been usually ignored in prior studies. Accordingly, there arises a necessity to address these voids in understanding. Here, it is imperative to undertake misalignment angle calculations through the integration of both the bearing and rotating unit. This approach ensures that the derived misalignment angles match with the actual situation, thereby avoiding over-exaggeration. Additionally, elucidating the determinants of misalignment is important. Furthermore, the researchers are looking to compare the results between rigid and flexible journal configurations to accurately describe the different effects of elastic journal deformation.

This paper introduces a coupled computational methodology aimed at exploring the performance of misaligned bearings while considering journal deformation and its interaction with bearing forces. The approach integrates the finite element method (FEM) to compute journal deformation and the finite difference method (FDM) to solve lubricant pressure governed by the Reynolds equation. Meshes generated via FEM and FDM are aligned axially to facilitate the coupling of journal deformation and bearing force. Subsequently, bearing performance is determined iteratively. A methodology for determining general misalignment angles within a rotor-bearing system is outlined based on geometric relationships and journal deformation. Finally, the study discusses the impact of bearing length-diameter ratio, rotation speed, and clearance on bearing performance and misalignment angles under different external loads.

2. Mathematical modeling

The comparison of the difference in the film characteristics for rigid and flexible journal deformation-induced misalignment is the main target of this study. Therefore, the following classical assumptions are made for the bearing model. First, it is provided that the lubricant is incompressible. Second, the thickness variation caused by bush deformation is neglected by assuming that the bearing bush is rigid and well-assembled on the base. Third, thermal conditions are considered since the lubricant viscosity is varied with temperature. However, the lubricant flow is assumed to adiabatic in thermal analysis, ignoring the heat conductivity between solid and lubricant.

The theoretical framework is outlined as follows. Firstly, the discussion addresses the determination of lubricant film thickness considering misalignment, as it serves as a fundamental aspect in resolving the lubrication performance of HDB. Subsequently, the generalized Reynolds equation, governing pressure and the energy equation, governing temperature, follow. Afterward, the methodology for determining journal deformation is elucidated.

2.1 Thickness of the lubricant film considering misalignment

The diagrams of lubricant flow in aligned, as well as misaligned with rigid and flexible journal situations, are sketched in Figure 1(a). As the fluid flows from flow Section 1 to 2, the pressure will increase due to the decreased flow area. Due to the misalignment, the flow sections are changed quite significantly and are modified even more if a flexible journal is considered. Once the magnitude of the journal's elastic deformation reaches the same magnitude as the film thickness, it will significantly influence the lubricant performance. Therefore, it is important to consider both, the misalignment and the flexible deformations, for

Figure 1 Diagram of the lubricant flow under different conditions (a), a misaligned HDB (b) and the projection of center-lines on the *yoz* and *xoy* plane (c)

(a)

(b)

(c)
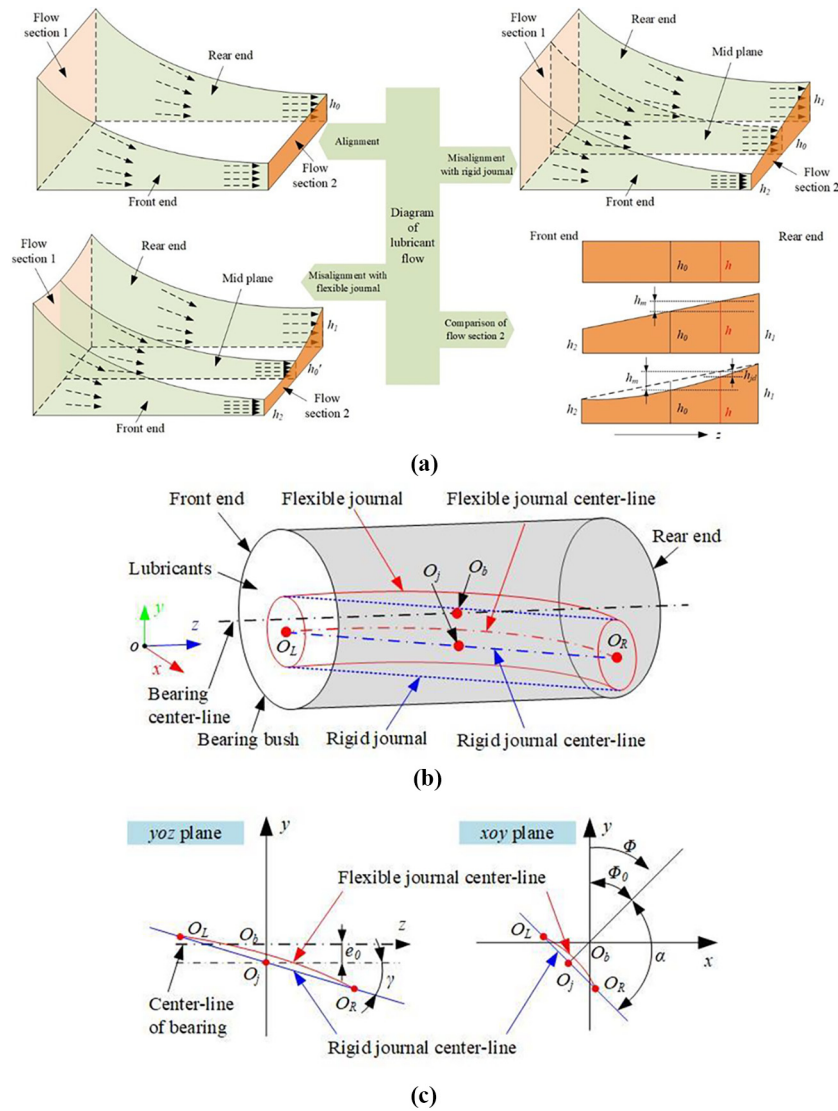
Notes: (a) Diagram of lubricant flow under different conditions; (b) diagram of a misaligned HDB; (c) projection of center-lines on *yoz* and *xoy* plane
Source: Author's own creation

the computation of the film thickness. To this aim, first, the geometry of a misaligned HDB is shown in Figure 1(b). The edge of the rigid journal is represented by blue dashed lines, while the edge of the flexible journal is depicted by red solid lines. The journal center of the left and right ends are denoted by O_L and O_R.

To describe the lubricant film thickness, the journal center-line is projected on the two perpendicular planes *yoz* and *xoy*, as shown in Figure 1(c). Here, the angles α and γ, between the rigid journal center-line and the coordinate axes are defined. Therefore, the lubricant thickness for the rigid situation is derived as (Yang *et al.*, 2022):

$$h = c + e_0\cos(\Phi\text{-}\Phi_0) + h_m, \qquad (1)$$

where c represents the clearance between the journal and bearing bush. e_0 denotes the eccentricity, i.e. the distance between the centers of the journal and bearing at mid-plane. Φ_0 stands for the attitude angle at mid-plane. h_m represent the thickness caused by misalignment, as (Sun *et al.*, 2014; Wang *et al.*, 2021):

$$h_m = \tan\gamma\left(y - \frac{L}{2}\right)\cos(\Phi\text{-}\alpha\text{-}\Phi_0), \qquad (2)$$

in which α and γ are the misaligned angles, as shown in Figure 1(c). These can be calculated by the coordinates of the journal end centers O_L and O_R according to geometric relationships (Ma *et al.*, 2018; Gu *et al.*, 2019). When the

flexibility of the journal is taken into account, the thickness variation caused by the journal deformation h_{jd} is added to the formulation of the lubricant film is modified to:

$$h = c + e_0\cos(\Phi\text{-}\Phi_0) + h_m + h_{jd}, \qquad (3)$$

The thickness variation h_m depends on axial and cylindrical coordinates. However, it is difficult to capture h_{jd} by an analytical function.

Therefore, the journal is divided into several parts along the axial direction. The exemplary section i is shown in Figure 2.

The eccentricity and attitude angle at the i-th section, denoted by e_i and Φ_{0i}, are calculated separately. Thus, the thickness is re-organized as:

$$h = c + e_i\cos(\Phi\text{-}\Phi_{0i}). \qquad (4)$$

For the aligned situation, the eccentricity position of the journal is constant along the axial direction. Thus, the eccentricity e_i and attitude angle Φ_{0i} for each section are constant. For the rigid journal situation considering misalignment, the eccentricity e_i and attitude angle Φ_{0i} are available through equation (2) or computations using the coordinates at two bearing ends.

The eccentricity e_i is composed of the basic eccentricity e_b and the deformation part e_{ui}, which are visualized on the right side of Figure 2. The basic part e_b represents the general position of the whole journal, while the deformation part e_{ui} quantifies the deformation-induced misalignment. Utilizing the components of $\{e_b, e_{ui}\}$ in the x- and y- direction, e_i is determined by Yang *et al.* (2023):

$$e_i = \sqrt{(e_{bx} + e_{uix})^2 + (e_{by} + e_{uiy})^2}. \qquad (5)$$

Correspondingly, the attitude angle is calculated by:

$$\Phi_{0i} = \text{atan}[(e_{bx} + e_{uix})/(e_{by} + e_{uiy})]. \qquad (6)$$

Once all constituents to compute the film thickness are available, the pressure can be computed by the generalized Reynolds equation.

2.2 Generalized Reynolds equation

Considering turbulence effects, the generalized Reynolds equation in cylindrical coordinates is derived under the steady condition, as (Constantinescu, 1962; Ng and Pan, 1965; Chun and Ha, 2001):

Figure 2 Diagram of the HDB considering the journal deformation
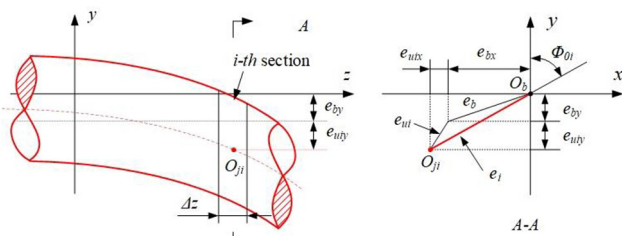
Source: Author's own creation

$$\frac{1}{R^2}\frac{\partial}{\partial\Phi}\left(\frac{h^3}{\mu}G_\Phi\frac{\partial p}{\partial\Phi}\right) + \frac{\partial}{\partial z}\left(\frac{h^3}{\mu}G_z\frac{\partial p}{\partial z}\right) = \frac{U}{2R}\frac{\partial h}{\partial\Phi}, \qquad (7)$$

where R stands for the bearing radius, p and h represent the pressure and thickness of the lubricant film, respectively, μ is the lubricant viscosity, and U is the rotational speed. G_Φ and G_z are turbulent factors, as:

$$\begin{cases} G_\Phi = \dfrac{1}{12(1 + 0.0136Re^{0.9})}, \\ G_z = \dfrac{1}{12(1 + 0.0043Re^{0.96})}, \end{cases} \qquad (8)$$

where $\text{Re} = {}^{\rho Uh}/_\mu$ is the Reynolds number, and ρ represents the density of the lubricant. For laminar flow, $G_\Phi = G_z = 12$. Then, the film pressure is found by solving the Reynolds equation using FDM. The bearing support forces are considered a cause of journal deformation. It is known that the pressure distribution is unsymmetrical due to the misalignment (Sun and Gui, 2004). Herein, the bearing force needs to be calculated at each section as:

$$\begin{Bmatrix} F_{xi} \\ F_{yi} \end{Bmatrix} = -\Delta z\int_0^{2\pi} p(\Phi, z)\begin{Bmatrix} \cos\Phi \\ \sin\Phi \end{Bmatrix}Rd\Phi, \qquad (9)$$

where Δz is the length of the section.

2.3 Energy equation

As the lubricant environment depends on the thermal conditions, the energy equation is described next to consider the effects of temperature variations on the lubricant performance as well. As such, the lubricant viscosity required in the Reynolds equation varies with temperature and is described by the following relationship (Shin *et al.*, 2021):

$$\mu = \mu_0 e^{(T-T_0)}, \qquad (10)$$

where T_0 is the reference temperature. The temperature field of the lubricant film is governed by the energy equation. According to the principle of energy conservation, the energy equation is derived as (Constantinescu, 1973; Safar and Szeri, 1974; Chun and Ha, 2001):

$$\rho\left[\left(\frac{Uh}{2} - \frac{h^3}{R\mu}G_\Phi\frac{\partial p}{\partial\Phi}\right)\frac{\partial(c_\nu T)}{R\partial\Phi} + \frac{h^3}{\mu}G_z\frac{\partial p}{\partial z}\frac{\partial(c_\nu T)}{\partial z}\right]$$
$$= \tau_c U + \left[G_\Phi\left(\frac{\partial p}{R\partial\Phi}\right)^2 + G_z\left(\frac{\partial p}{\partial z}\right)^2\right], \qquad (11)$$

where c_ν is the specific heat of the lubricant, and τ_c represents the Couette shear stress. The heat exchange within the lubricant to the surroundings is neglected for the above energy equation. (2)0.4 Boundary condition.

The Reynolds boundary condition (Qiu, 1995; Sun *et al.*, 2014; Zheng *et al.*, 2022) is adopted to solve the Reynolds equation in this work. The pressure at the bearing ends, i.e. $z = 0$ and $z = L$, is set to zero. The pressure gradient is zero at the trailing edge of the positive region in the circumferential direction., i.e.:

$$\begin{cases} p = 0 \text{ at } z = 0, L, \\ p = 0 \text{ at } \Phi = 0, \theta_c \leq \Phi \leq 2\pi, \\ p = \dfrac{\partial p}{\partial \Phi} = 0 \text{ at } \Phi = \theta_c, \end{cases} \quad (12)$$

where θ_c indicates the angle where the film ruptures. Notably, the pressure is assigned to zero in the cavitation region (Zhu *et al.*, 2020). The following boundary condition is adopted to solve the energy equation (Sharma *et al.*, 2019; Dhanola and Garg, 2020):

$$T = T_0 \text{ at } \Phi = 0. \quad (13)$$

These conditions are subsequently used in the expression of the film thickness and governing equations of lubrication properties as given in Sections 2.1–2.3. The following section describes the flexible journal deformation as it is required for equations (5) – (6).

2.5 Rotor modeling and bending deformation

To determine the journal deformation, a Timoshenko beam element-based FEM is utilized to model the rotor (Gayen *et al.*, 2017; Han and Ding, 2018; Briend *et al.*, 2020). A two-node Timoshenko beam element is adopted to model the rotor, where each node has four degrees of freedom (Nelson, 1980). As shown in Figure 3, $\{u_i, v_i\}$ ($i = 1, 2$) represent the translational displacements of the two end nodes along the x- and y- directions, and $\{\theta_i, \beta_i\}$ ($i = 1, 2$) represent the rotational displacements of two end nodes around the x- and y- axes.

Considering operating conditions and the material of the journal, the deformation is generally quite small (Sun *et al.*, 2014). Thus, only elastic deformation is considered in this study. The journal deformation caused by an external load is described by:

$$\{F\} = [K]\{d\}, \quad (14)$$

where $[K]$ is the stiffness matrix, $\{F\}$ and $\{d\}$ represent the vectors of the external load and deformation.

Then, the bending deformation is calculated by solving equation (14) (Özütok and Madenci, 2017; Aldousari, 2017). Subsequent to the theoretical exposition, the subsequent

Figure 3 Sketch of a Timoshenko beam element
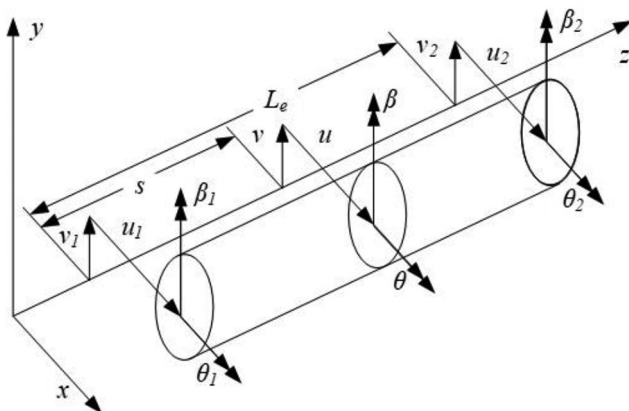
Source: Author's own creation

section explains the numerical solution in accordance with the established theory.

3. Numerical algorithm

Section 2 details the methods for calculating both the bearing force and journal deformation. Here, it is found that the components of the eccentricities $\{e_b, e_{ui}\}$ in x- and y- direction are fundamental to determining the bearing forces. However, the components of eccentricity are based on the journal deformation, which in turn depends on the bearing force. Thus, the bearing force has to be determined before the eccentricities can be calculated and vice versa. Therefore, an interactive algorithm is developed in this section considering the interactions between the bearing force and journal deformation.

3.1 Scheme of the interaction between eccentricities and bearing forces

A rotor-bearing model, as shown in Figure 4, is adopted for the numerical simulation in this study. The rotor is represented by a simplified model of a rotating system structure, which is widely used in applications such as centrifugal pumps or compressors, engines, mixers, and propulsion systems of ships (Kippers *et al.*, 2010; Tkachuk *et al.*, 2021; Lu *et al.*, 2022; He *et al.*, 2022). The external loads are mainly applied at one end of the rotor. The rotor is generally supported by hydrodynamic bearings or combined with roller bearings. As excitations forces loads by the lubricant film support and gravity forces from the bearing and rotor are applied.

To calculate the pressure distribution by an FDM, the lubricant film is represented by a two-dimensional finite difference mesh and is divided into a $m \times n$ grid (Ebrat *et al.*, 2004; Zhang *et al.*, 2019). To establish the interactive relationship between the bearing force and the journal deformation, the journal is meshed by FEM with m elements along the length of the rotor, which matches the finite difference mesh, as shown in Figure 4. Bearing forces in each section are obtained by equation (9) and applied to the corresponding nodes to calculate the journal deformation by the relations established in section 2.5. In turn, the calculated journal deformation is used to re-calculate the eccentricities and to update the bearing forces by equations (4) – (10). An equilibrium position is obtained by an iterative process.

Figure 4 Sketch of a cantilever rotor-bearing system
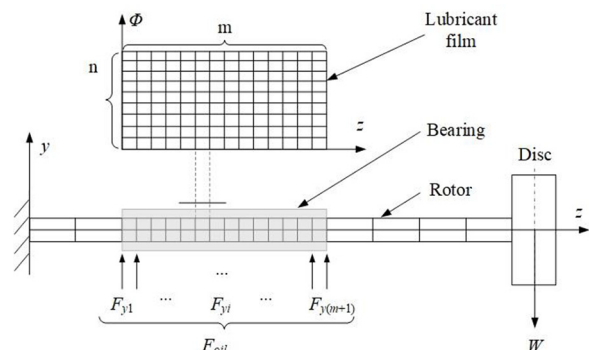
Source: Author's own creation

3.2 Equilibrium position

The bearing forces are functions of the eccentricity e and the rotation speed Ω (i.e. $F_{bk} = F_{bk}(e, \Omega)$, $k = x, y$). Meanwhile, the bearing forces balance the static external load W (i.e. $F_x = 0$ & $F_y = W$ for a horizontal rotor) in the equilibrium position (Krämer, 2013; He *et al.*, 2014). The total bearing forces are the sum of the bearing forces at all sections, and equal to the static external load at the equilibrium position, as:

$$F_x = \sum_{i=1}^{m+1} F_{xi} = 0, \quad F_y = \sum_{i=1}^{m+1} F_{yi} = W, \tag{15}$$

where m represents the number of divided sections of the oil-film in the axial direction. The static external load W is a constant value for a steadily operating rotor-bearing system. Therefore, the eccentricity e in the equilibrium position can be determined for a certain rotation speed Ω (Visnadi and de Castro, 2019).

When considering a deformation-induced misalignment, the equilibrium between bearing forces and the static load is disrupted if the basic eccentricity e_b remains fixed at the same value e as in the aligned state. This disparity arises from pressure variations resulting from the presence of the deformed eccentricity e_{ui}. Therefore, e_b and e_{ui} need to be determined in an interactive way to capture the equilibrium position.

In this way, a numerical procedure is used to determine e_b and e_{ui} utilizing a triple-layer loop structure depicted in the flowchart in Figure 5. The inner loop determines the pressure distribution. In the intermediate loop, the pressure distribution is applied to compute the bearing forces. These are subsequently used to determine the deformed eccentricity e_{ui}. The outer loop is used to capture the basic eccentricity e_b. The stopping condition of the intermediate loop is defined according to the convergence of the bearing force, which may not equal the external load. The convergence criterion for the outer loop is determined based on the balance between bearing force and external load, as shown in equation (14). With the determination of e_b and e_{ui} at the equilibrium position, the interactive performance is obtained. In Figure 5, δ_j and Δ_j ($j = x, y$) represent the convergence limits in the intermediate and outer loop, respectively. In this study, δ_j is set as 0.01, whereas Δ_j ($j = x, y$) equals $0.01\,W$ to improve the computational efficiency. The convergence of the Reynolds equation and energy equation is defined as:

$$\sum_{i=1}^{m} \sum_{j=1}^{n} \left| \frac{p_{i,j}^{l+1} - p_{i,j}^{l}}{p_{i,j}^{l}} \right| \le 1e-5, \quad \sum_{i=1}^{m} \sum_{j=1}^{n} \left| \frac{T_{i,j}^{l+1} - T_{i,j}^{l}}{T_{i,j}^{l}} \right| \le 1e-5, \tag{16}$$

where l represents the iteration loop.

In this study, a Matlab code is developed to realize the interactive algorithm. First, the FEM and FDM programs are established according to section 2. Second, the interactive program is developed to connect the FEM and FDM. The details of FDM and FEM are refereed in the work of Ebrat *et al.* (2004) and Nelson (1980).

4. Validation

The experimental and theoretical results presented by Ferron *et al.* (1983) are used to validate the calculation method in this study. Table 1 lists the parameters of the bearing used in the test rig. A mesh convergence study for the mesh of FDM is carried out. The results are presented in Table 2, which shows the maximum pressure achieves convergence for the given mesh grids. The mesh grid with 20 elements axially and 180 elements circumferentially is used for subsequent study.

The pressure and temperature in the mid-plane of the bearing are presented in Figure 6. It is observed that the pressure shows a good agreement, but the agreement with the temperature is not very satisfactory. In addition, the temperature at the boundary of the oil inlet is discontinuous. The difference in

Figure 5 Flowchart of analysis for interactive performance
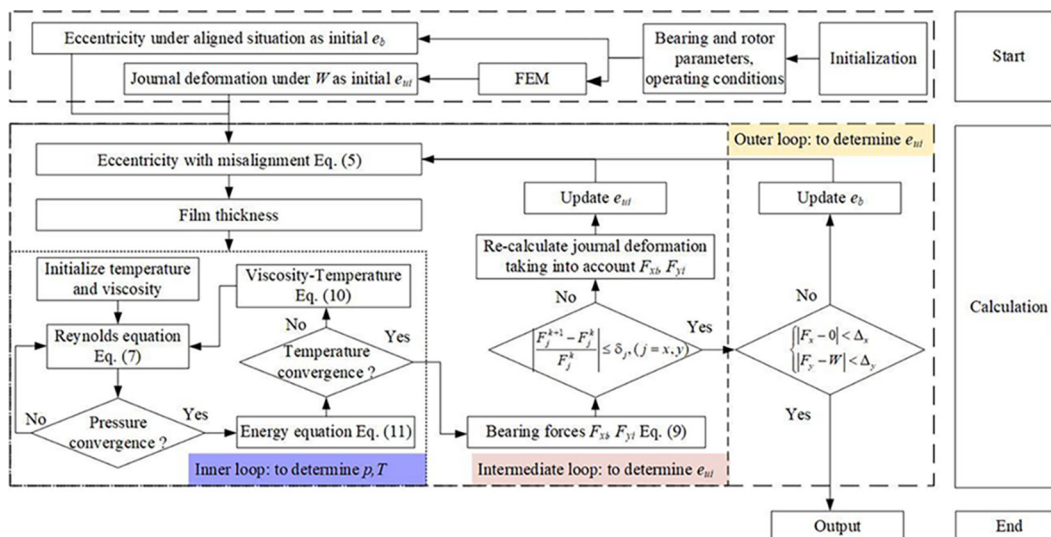
Source: Author's own creation

Table 1 Parameters and running conditions of the bearing presented by Ferron *et al.* (1983)

Description	Value
Bearing length (*L*)	8e-3 m
Journal radius (*R*)	5e-3 m
Clearance (*c*)	0.152e-3 m
Lubricant density (ρ)	860 kg/m^3
Viscosity at 40°C (μ_0)	0.0277 Ns/m^2
Rotation speed (Ω)	2000 rpm
Specific heat (c_v)	2000 J/(kg°C)
Inlet oil temperature (T_0)	40°C

Source: Authors' own creation

Table 2 A mesh convergence study for the mesh grid of FDM

Mesh grid ($m \times n$)	20 × 90	20 × 120	20 × 180	20 × 240
Maximum pressure (MPa)	1.5490	1.5504	1.5518	1.5525
Mesh grid ($m \times n$)	20 × 90	20 × 120	20 × 180	20 × 240
Maximum pressure (MPa)	1.5435	1.5449	1.5463	1.5470

Source: Authors' own creation

temperature might be caused by two aspects. First, the assumption that the lubricant is considered as adiabatic neglects the heat exchange between the lubricant and its surroundings (Zhu *et al.*, 2020; Feng *et al.*, 2019). Second, the mixed temperature of the inlet and re-circulating lubricant flow is neglected, which causes the different temperatures at the start and end points of the circumferential direction. Figure 6(c) gives the comparison of dimensionless temperature in mid-plane between the present work and Jang and Chang (1988) which considered the adiabatic flow. It shows the results have good agreement. Since the misalignment is ignored in the work of Ferron *et al.* (1983) and Jang and Chang (1988), further validation for the proposed framework will be implemented in future work.

5. Results and discussion

To illustrate the influence of the deformation-induced misalignment on the performance of the HDB, a numerical study is conducted. First, the interactive performance of the rotor-bearing system based on the proposed formulation and verified method is discussed. The effects of the bearing length-diameter ratio, rotation speed, and clearance on the interactive performance are subsequently investigated.

5.1 Performance under interaction

The parameters used to study the performance under the interaction of a cantilever rotor-bearing system are listed in Table 3. For the convenience of subsequent parameter studies, hereby, the journal length and clearance are described as ratios with respect to journal diameter and radius, respectively. The pressure and thickness distributions of the oil film are analyzed. To explain the influence of misalignment on the performance

Figure 6 Comparison of pressure and temperature in mid-plane between present work and Ferron *et al.* (1983) and Jang and Chang (1988)

(a)

(b)

(c)
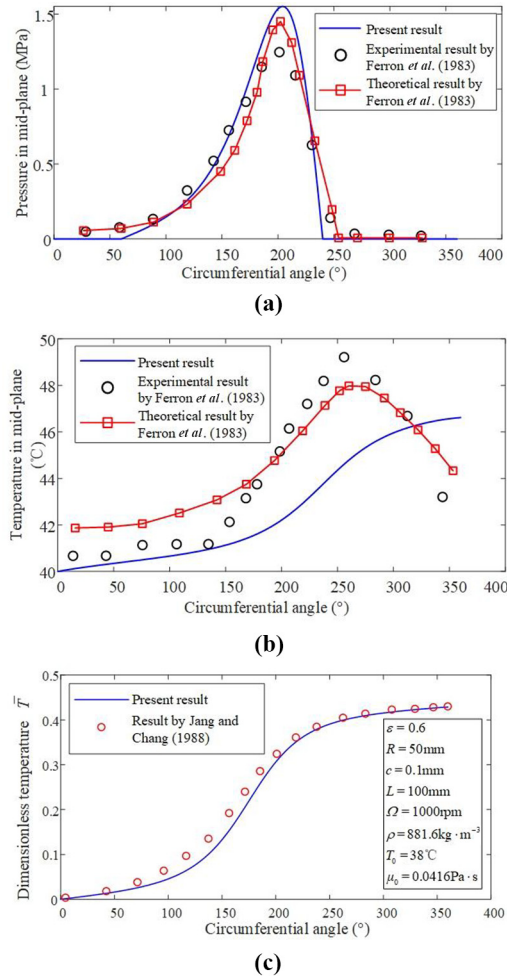
Notes: (a) Comparison of pressure in mid-plane between present work with Ferron *et al.* (1983); (b) comparison of temperature in mid-plane between present work with Ferron *et al.* (1983); (c) comparison of temperature in mid-plane between present work with Jang and Chang (1988)
Source: Author's own creation

Table 3 Parameters of the rotor and bearing

| Description	Value
Journal radius (*R*)	0.1 m
Length-diameter ratio (*L/D*)	0.7
Lubricant density (ρ)	860 kg/m^3
Clearance-radius ratio (*c/R*)	3.9837e-3
Viscosity at 40°C (μ_0)	0.0236 Ns/m^2
Rotation speed (Ω)	1,200 rpm
Static external load (*W*)	70 kN
Specific heat (c_v)	2,000 J/(kg°C)

Source: Authors' own creation

of the bearing, the result in the aligned situation is also calculated for comparison.

Figure 7 shows the calculation results of the bearing in the aligned and misaligned situations for the same rotation speed and external load. From Figure 7(a) to 7(d), it is observed that thickness and pressure become unsymmetrical along the z direction when considering the misalignment. The minimum thickness in the misaligned situation is smaller than that in the aligned situation. On the contrary, the pressure becomes larger than in the aligned situation. The maximum pressure moves away from the mid-plane. This phenomenon shows the same tendency as previous research (Bouyer and Fillon, 2002; Sun and Gui, 2004; Xu *et al.*, 2015), which illustrates that the misalignment is essential to be taken into consideration.
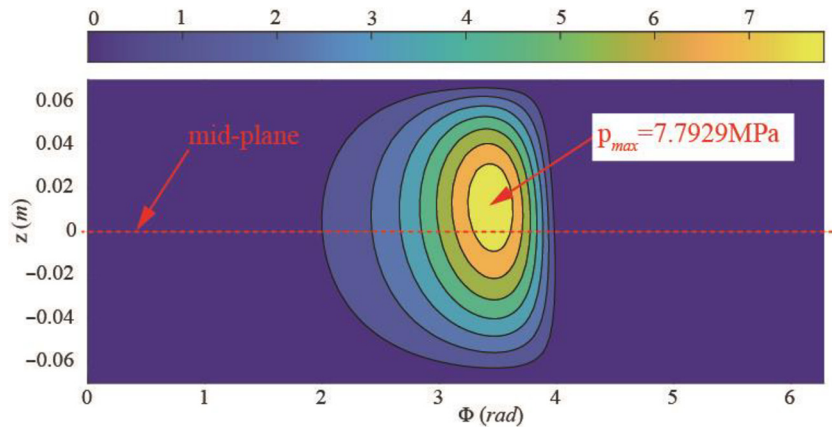
The pressure distribution and pressure in the mid-plane under rigid and flexible journal conditions are plotted in Figure 8. It is

Figure 7 Comparison of film thickness and pressure distribution between aligned and misaligned situations
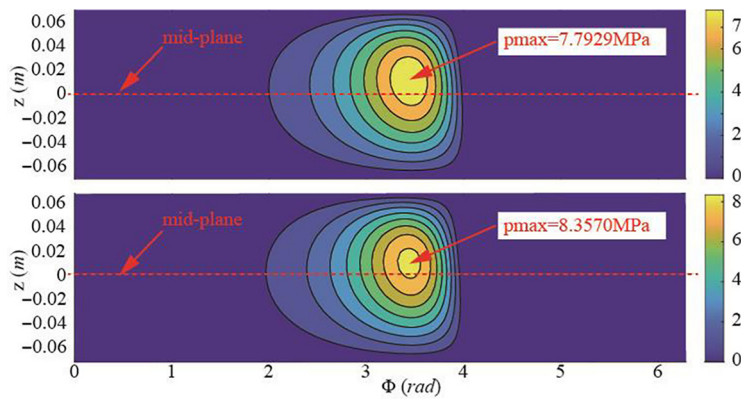

(a)

(b)

(c)
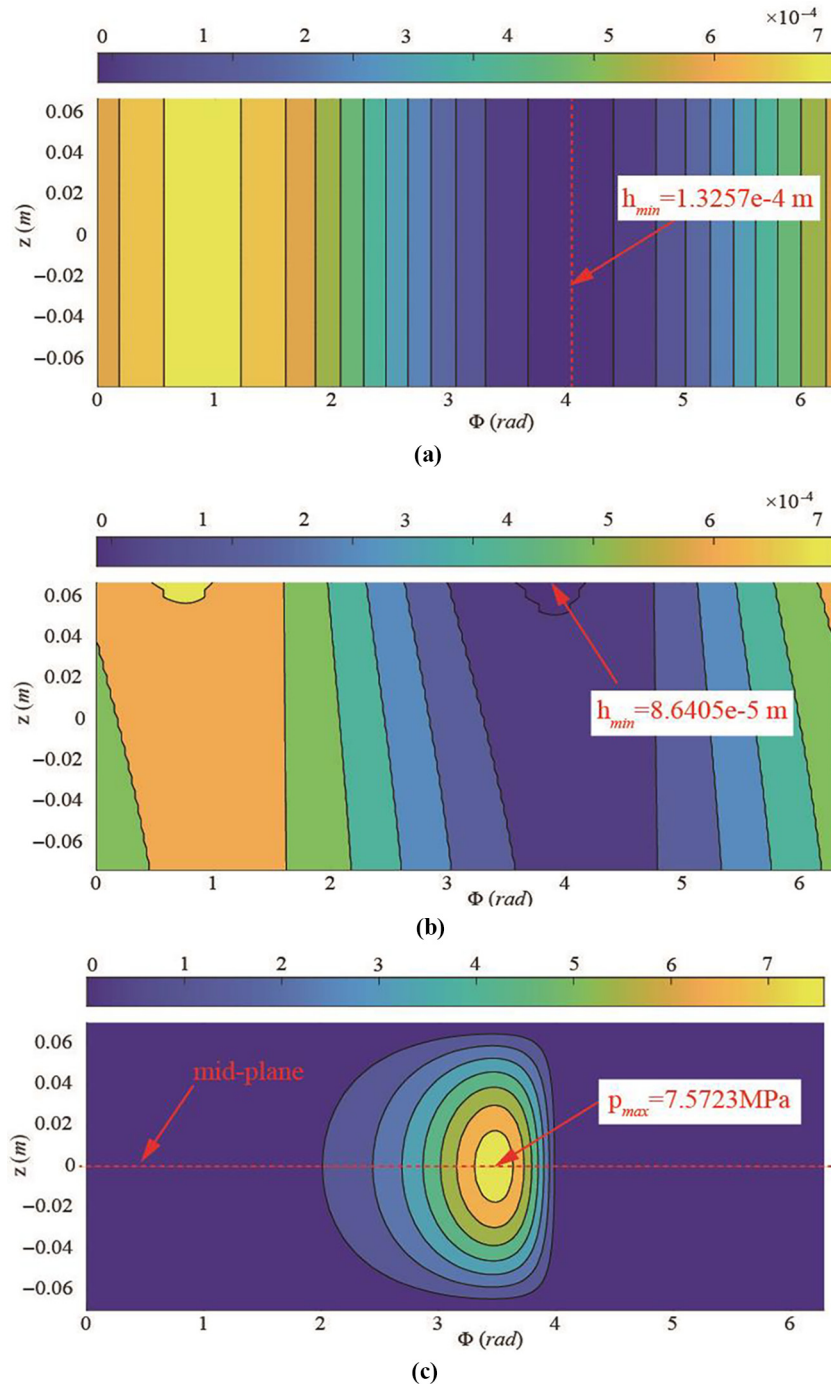
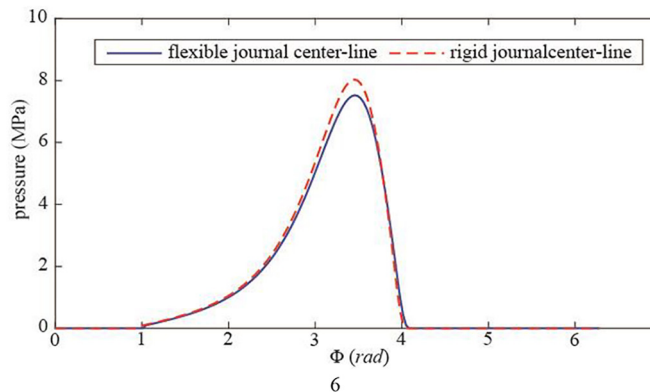(*continued*)

Figure 7

(d)

Notes: (a) Film thickness under aligned situation; (b) film thickness under misaligned situation; (c) film pressure under aligned situation; (d) film pressure under misaligned situation
Source: Author's own creation

Figure 8 Comparison of pressure distribution and pressure in mid-plane between rigid and flexible journal conditions

(a)

6

(b)

Notes: (a) Pressure distributions: rigid (upper) and flexible (lower) journal situation; (b) pressure in mid-plane
Source: Author's own creation

observed that there is an evident difference under these two conditions, in which the difference in maximum pressure is 7.24%. This indicates that the thickness contributed by the journal deformation has a non-negligible influence on the bearing performance. According to the geometry relationship as shown in Figure 1(b), the misaligned angles are obtained as $\gamma = 0.0445°$ and $\alpha = 130.76°$.

5.2 Effect of length-diameter ratio

Figure 9 shows the comparison of maximum pressure between rigid and flexible journal situations under different length-diameter ratios. From Figure 9(a), it is noticed that the maximum pressure decreases as the length-diameter ratio increases. At the same time, the increment of the static load W causes an increment of the maximum pressure. The maximum pressure under the rigid journal situation is generally smaller than in the flexible condition. The increment of the maximum pressure is caused by the strengthened hydrodynamic effect since the lubricant film becomes thinner as the static load increases (Lund and Thomsen, 1978). On the other hand, the bearing loading capacity is enhanced as the length-diameter ratio increases. For the same static load, the larger the effective inner area of the bearing, the smaller the pressure required. Accordingly, the maximum pressure decreases as the length-diameter ratio decreases. The difference between the flexible and rigid settings is visualized in Figure 9(b). It is observed that

the difference decreases with the increasing length-diameter ratio. Furthermore, the difference becomes greater as the static load W increases. The thickness becomes thinner for the heavier static load for both rigid and flexible situations. In addition, the thickness of the flexible situation is thinner than the rigid situation. Thus, the increment of the maximum pressure in the flexible situation is more significant than in the rigid situation. Therefore, the difference in maximum pressure increases as the static load increases. Meanwhile, the increment of the length-diameter ratio leads to an increment of thickness as well. Therefore, the difference in maximum pressure decreases as the length-diameter ratio increases.

The misaligned angles under different length-diameter ratios are calculated as shown in Figures 9(c) and 9(d). It is suggested that γ generally increases as the length-diameter ratio increases, while α shows the opposite tendency. However, γ and α both become larger for larger static loads. This is due to the fact that a heavier load causes larger journal deformation. In addition, the increments of the static load and length-diameter ratio cause a decrease in the attitude angle (Lund and Thomsen, 1978; Dyk *et al.*, 2019). Thus, it is indicated by Figure 1(b) that α increases as the attitude angles decrease.

5.3 Effect of rotation speed

Figure 10 shows the comparison of maximum pressure between rigid and flexible journal situations under different

Figure 9 Maximum pressure of rigid and flexible journal situations and misaligned angle γ and α versus length-diameter ratio
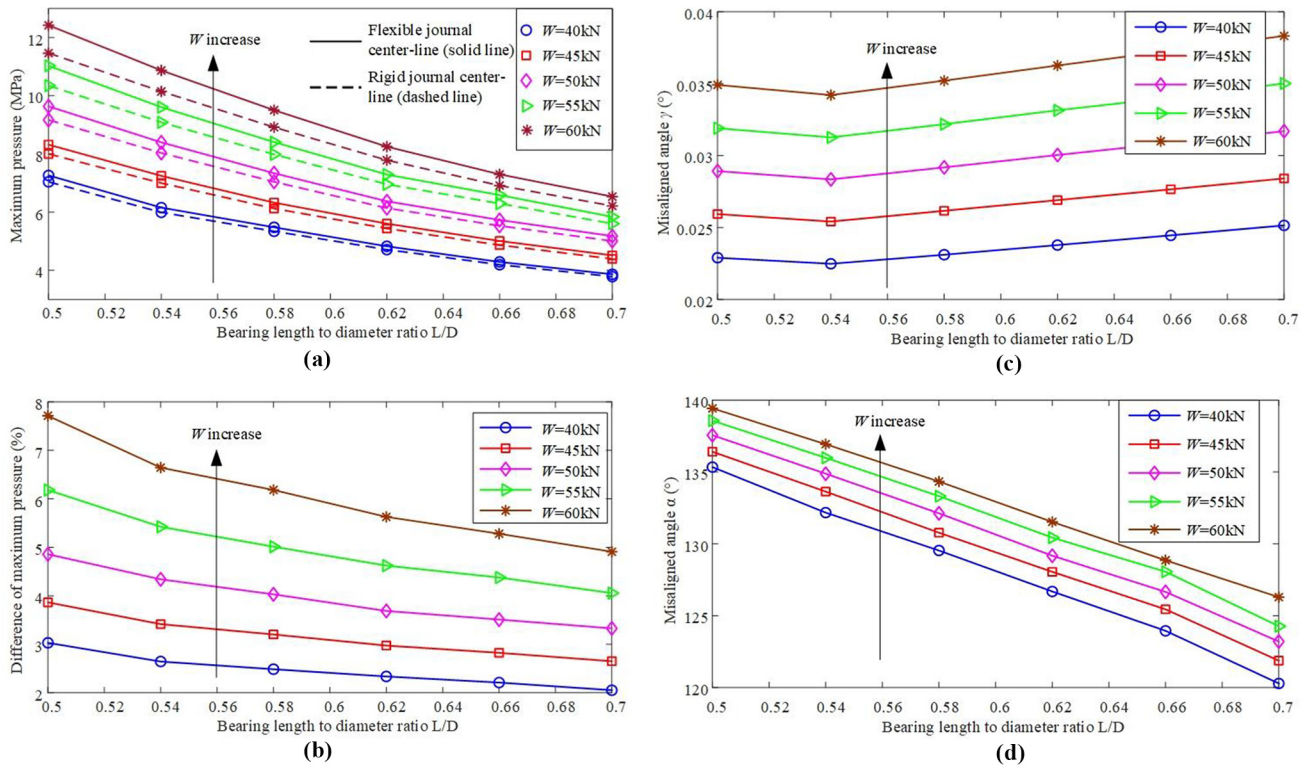
Notes: (a) Maximum pressures; (b) difference of maximum pressures between rigid and flexible journal situations; (c) misaligned angle γ; (d) misaligned angle α
Source: Author's own creation

Figure 10 Maximum pressure of rigid and flexible journal situations and misaligned angle γ and α versus rotation speed
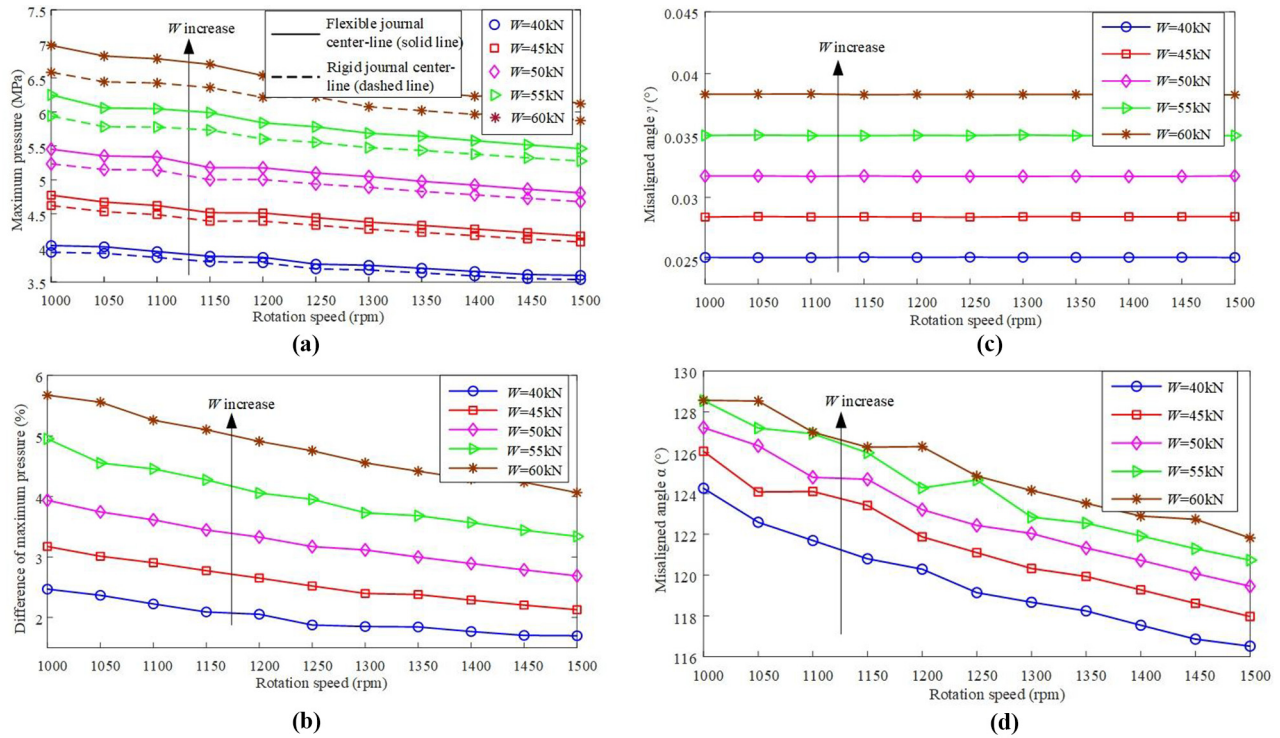
Notes: (a) Maximum pressures; (b) difference of maximum pressures between rigid and flexible journal situations; (c) misaligned angle γ; (d) misaligned angle α
Source: Author's own creation

rotation speeds. From Figure 10(a), it is noticed that the maximum pressure decreases as the rotation speed increases. At the same time, the increment of the static load causes an increment of the maximum pressure. The lubricant thickness becomes thicker as the rotation speed increases due to the enhancement of the hydrodynamic effect for the same static load. Thus, the pressure declines as the thickness increases. Similarly, the lubricant thickness becomes thicker as the static load decreases, leading to the same tendency. The maximum pressure in the rigid journal situation is generally smaller than in the flexible case. The maximum pressure difference decreases with the increasing rotation speed as shown in Figure 10(b). The rotation speed has the same influence on the difference between the flexible and rigid journal setting as the length-diameter ratio because their increments both increase the thickness. Meanwhile, it is observed that the difference between the flexible and rigid journal situations becomes larger as the static load increases, which is similar to the illustration in Sec 5.2.

The misaligned angles are calculated under different rotation speeds, as shown in Figures 10(c) and 10(d). It is suggested that γ and α both become greater as the static load increases. In addition, α keeps a decreasing tendency as the rotation speed increases. This is due to the fact that the attitude angle decreases as the rotation speed increases (Krämer, 2013). However, the rotation speed has little influence on the elastic deformation of the journal.

5.4 Effect of clearance
Figure 11 shows the comparison of the maximum pressure between rigid and flexible journal situations under different clearance-radius ratios. From Figure 11(a), it is noticed that the increment of the static load causes an increment of the maximum pressure. There is merely a slight increase in maximum pressure as the clearance-radius ratio increases. The maximum pressure in the rigid journal situation is generally smaller than in the flexible case. The difference between these two situations is given in Figure 11(b). It is observed that the difference becomes greater as the static load increases. However, the increasing clearance-radius ratio has a slight influence on the difference between the rigid and flexible situation in maximum pressure. This is due to the fact that the magnitude of the journal deformation achieves the same magnitude as the clearance. Therefore, the clearance-radius ratio in the given condition has limited influence on the hydrodynamic effect compared with the impact of the misalignment. This finding is consistent with the observation in previous studies that the influence of clearance on lubricant performance is smaller than other factors (Prashad, 1988; Simmons and Dixon, 1994).

The misaligned angles under different clearance-radius ratios are calculated as shown in Figures 11(c) and 11(d). It is suggested that γ and α both become greater as the static load increases. At the same time, the clearance-radius ratio has negligible influence on γ, while α increases as the clearance-radius ratio increases. This is owing to the fact that the

Figure 11 Maximum pressure of rigid and flexible journal situations and misaligned angle γ and α versus clearance-radius ratio

(a)

(b)

(c)
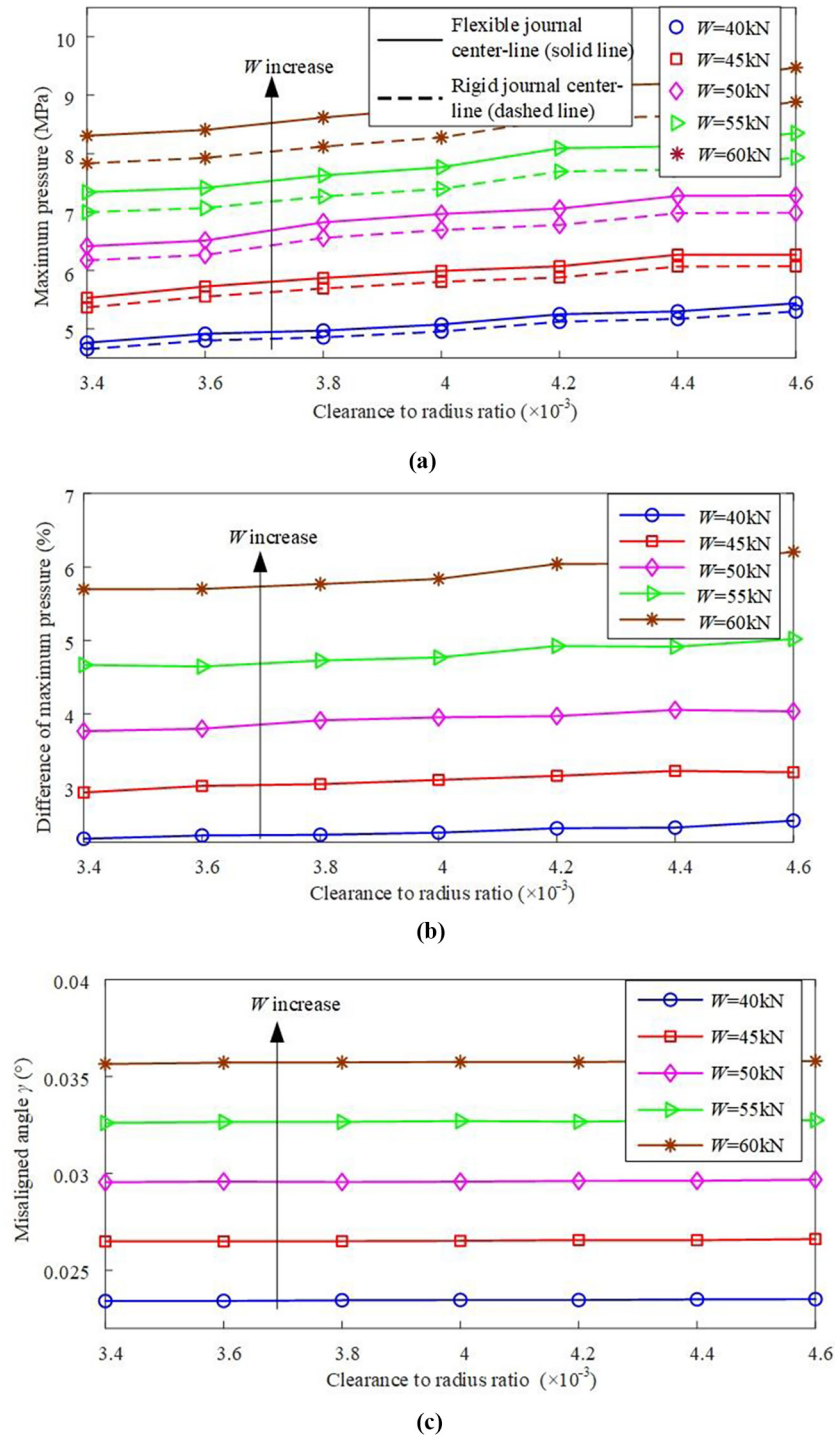
(*continued*)

Figure 11
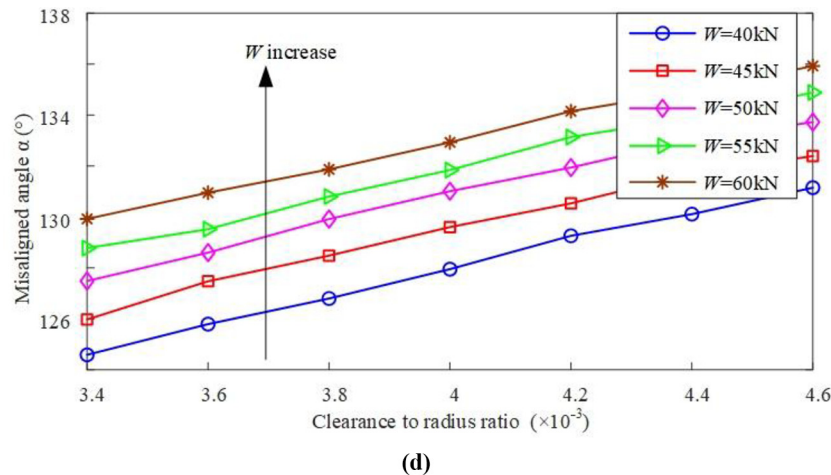
(d)

Notes: (a) Maximum pressures; (b) difference of maximum pressures between rigid and flexible journal situations; (c) misaligned angle γ and (d) misaligned angle α
Source: Author's own creation

increment of the clearance-radius ratio causes a change of the position of the journal center, leading to a change of attitude angle. However, this has little influence on the elastic deformation of the journal.

6. Conclusions

The difference between considering a rigid and flexible journal on the performance of a deformation-induced misaligned HDB is investigated in this work. The interaction between the journal deformation and the bearing force is taken into account by alternating FEM and FDM until the equilibrium position is reached. By calculation, the following conclusions are drawn:

· The influence of the elastic deformation of the journal needs to be considered since the hydrodynamic effect is significantly changed compared with the rigid journal situations. The difference between considering rigid and flexible journals increases as the hydrodynamic effect is strengthened.
· The degree of misalignment depends on the difference in deformation at the journal ends, which is mainly related to the external load and journal length. This provides a reference for selecting appropriate bearings for rotating systems with known loads. The misalignment angle in the circumferential direction is affected by rotation speed, external load, journal length, and clearance since the attitude angle varies with these factors.

This study provides insight into the performance of a journal bearing under deformation-induced misalignment. In addition, the developed framework with the FEM-based model serves as a basis for the calculation of the dynamic response of the system, which will be investigated in future work.

References

Abass, B.A. and Kadhim, M.M. (2013), "Thermo-hydrodynamic analysis of misaligned journal bearing considering surface roughness and non-Newtonian effects", *Journal of Engineering*, Vol. 19 No. 5, pp. 637-653.

Abdou, K.M. and Saber, E. (2020), "Effect of rotor misalignment on stability of journal bearings with finite width", *Alexandria Engineering Journal*, Vol. 59 No. 5, pp. 3407-3417.

Aldousari, S.M. (2017), "Bending analysis of different material distributions of functionally graded beam", *Applied Physics A*, Vol. 123 No. 4, p. 296.

Bouyer, J. and Fillon, M. (2002), "An experimental analysis of misalignment effects on hydrodynamic plain journal bearing performances", *Journal of Tribology*, Vol. 124 No. 2, pp. 313-319.

Briend, Y., Dakel, M., Chatelet, E., Andrianoely, M.A., Dufour, R. and Baudin, S. (2020), "Effect of multifrequency parametric excitations on the dynamics of on-board rotor-bearing systems", *Mechanism and Machine Theory*, Vol. 145, p. 103660.

Buckholz, R.H. and Lin, J.F. (1986), "The effect of journal bearing misalignment on load and cavitation for non-Newtonian lubricants", *Journal of Tribology*, Vol. 108 No. 4, pp. 645-654.

Chun, S.M. and Ha, D.H. (2001), "Study on mixing flow effects in a high-speed journal bearing", *Tribology International*, Vol. 34 No. 6, pp. 397-405.

Constantinescu, V.N. (1962), "Analysis of bearings operating in turbulent regime", *Journal of Basic Engineering*, Vol. 84 No. 1, pp. 139-151.

Constantinescu, V.N. (1973), "Basic relationships in turbulent lubrication and their extension to include thermal effects", *Journal of Lubrication Technology*, Vol. 95 No. 2, pp. 147-154.

Dal, A. and Karaçay, T. (2017), "Effects of angular misalignment on the performance of rotor-bearing systems supported by externally pressurized air bearing", *Tribology International*, Vol. 111, pp. 276-288.

Dhanola, A. and Garg, H.C. (2020), "Thermohydrodynamic (THD) analysis of journal bearing operating with bio-based

nanolubricants", *Arabian Journal for Science and Engineering*, Vol. 45 No. 11, pp. 9127-9144.

Dick, A., Lin, C., Wang, Y. and Wang, Q.J. (2004), "Thermal validation of a misaligned grease-lubricated journal bearing model", *Proceedings of the Institution of Mechanical Engineers, Part J: Journal of Engineering Tribology*, Vol. 218 No. 5, pp. 423-435.

Dyk, Š., Rendl, J., Byrtus, M. and Smolík, L. (2019), "Dynamic coefficients and stability analysis of finite-length journal bearings considering approximate analytical solutions of the Reynolds equation", *Tribology International*, Vol. 130, pp. 229-244.

Ebrat, O., Mourelatos, Z.P., Vlahopoulos, N. and Vaidyanathan, K. (2004), "Calculation of journal bearing dynamic characteristics including journal misalignment and bearing structural deformation", *Tribology Transactions*, Vol. 47 No. 1, pp. 94-102.

Feng, H., Jiang, S. and Ji, A. (2019), "Investigations of the static and dynamic characteristics of water-lubricated hydrodynamic journal bearing considering turbulent, thermohydrodynamic and misaligned effects", *Tribology International*, Vol. 130, pp. 245-260.

Ferron, J., Frene, J. and Boncompain, R. (1983), "A study of the thermohydrodynamic performance of a plain journal bearing comparison between theory and experiments", *Journal of Lubrication Technology*, Vol. 105 No. 3, pp. 422-428.

Gayen, D., Chakraborty, D. and Tiwari, R. (2017), "Finite element analysis for a functionally graded rotating shaft with multiple breathing cracks", *International Journal of Mechanical Sciences*, Vol. 134, pp. 411-423.

Gu, T., Jane Wang, Q., Xiong, S., Liu, Z., Gangopadhyay, A. and Liu, Z. (2019), "Profile design for misaligned journal bearings subjected to transient mixed lubrication", *Journal of Tribology*, Vol. 141 No. 7, p. 071701.

Guo, H., Bao, J., Zhang, S. and Shi, M. (2022), "Experimental and numerical study on mixed lubrication performance of journal bearing considering misalignment and thermal effect", *Lubricants*, Vol. 10 No. 10, p. 262.

Han, B. and Ding, Q. (2018), "Forced responses analysis of a rotor system with squeeze film damper during flight maneuvers using finite element method", *Mechanism and Machine Theory*, Vol. 122, pp. 233-251.

He, T., Zou, D., Lu, X., Guo, Y., Wang, Z. and Li, W. (2014), "Mixed-lubrication analysis of marine stern tube bearing considering bending deformation of stern shaft and cavitation", *Tribology International*, Vol. 73, pp. 108-116.

He, T., Xie, Z., Ke, Z., Dai, L., Liu, Y., Ma, C. and Jiao, J. (2022), "Theoretical study on the dynamic characteristics of marine stern bearing considering cavitation and bending deformation effects of the shaft", *Lubricants*, Vol. 10 No. 10, p. 242.

Huang, Q. and Yan, X. (2020), "Impact factors on lubricant performance of stern bearing with misalignment angle induced by transverse vibration of shaft", *Ocean Engineering*, Vol. 216, p. 108051.

Jang, J.Y. and Chang, C.C. (1988), "Adiabatic analysis of finite width journal bearings with non-Newtonian lubricants", *Wear*, Vol. 122 No. 1, pp. 63-75.

Jang, J.Y. and Khonsari, M.M. (2015), "On the characteristics of misaligned journal bearings", *Lubricants*, Vol. 3 No. 1, pp. 27-53.

Kippers, N., Holloway, G. and Gerber, A. (2010), "Towards a model of vibration for a cantilevered mixing rotor", In Fluids Engineering Division Summer Meeting, Vol. 54518, pp. 599-611.

Krämer, E. (2013), *Dynamics of Rotors and Foundations*, Springer Science Business Media.

Lahmar, M., Frihi, D. and Nicolas, D. (2002), "The effect of misalignment on performance characteristics of engine main crankshaft bearings", *European Journal of Mechanics-A/Solids*, Vol. 21 No. 4, pp. 703-714.

Lu, J., Zhang, X., Pan, X. and Zhang, M. (2022), "Research on unbalanced vibration suppression method for coupled cantilever dual-rotor system", *Machines*, Vol. 10 No. 9, p. 758.

Lund, J.W. and Thomsen, K.K. (1978), "A calculation method and data for the dynamic coefficient of oil lubricated journal bearing", ASME Design Engineering Conference, Chicago, IL, ASME pub No. 100118, pp. 1-28.

Ma, X., Xu, W., Zhang, X. and Yang, F. (2018), "Effect of form errors on oil film characteristics of hydrodynamic journal bearings based on small displacement Torsor theory", *Industrial Lubrication and Tribology*, Vol. 71 No. 3, pp. 426-439.

Mallya, R., Shenoy, S.B. and Pai, R. (2017), "Static characteristics of misaligned multiple axial groove water-lubricated bearing in the turbulent regime", *Proceedings of the Institution of Mechanical Engineers, Part J: Journal of Engineering Tribology*, Vol. 231 No. 3, pp. 385-398.

Nelson, H.D. (1980), "A finite rotating shaft element using Timoshenko beam theory", *Journal of Mechanical Design*, Vol. 102 No. 4, pp. 793-803.

Ng, C.W. and Pan, C.H.T. (1965), "A linearized turbulent lubrication theory", *Journal of Basic Engineering*, Vol. 87 No. 3, pp. 675-682.

Ouyang, W., Liu, Q., Xiao, J., Huang, J., Zhang, Z. and Wang, L. (2023), "Experimental study on the distributed lubrication characteristics of full-size water-lubricated stern bearings under hull deformation", *Ocean Engineering*, Vol. 267, p. 113226.

Özütok, A. and Madenci, E. (2017), "Static analysis of laminated composite beams based on higher-order shear deformation theory by using mixed-type finite element method", *International Journal of Mechanical Sciences*, Vol. 130, pp. 234-243.

Prashad, H. (1988), "The effects of viscosity and clearance on the performance of hydrodynamic journal bearings", *Tribology Transactions*, Vol. 31 No. 2, pp. 303-309.

Qiu, Z.L. (1995), "A theoretical and experimental study on dynamic characteristics of journal bearings", Dissertation, University of Wollongong.

Ram, N. and C. Sharma, S. (2014), "Influence of wear on the performance of hole-entry hybrid misaligned journal bearing in turbulent regime", *Industrial Lubrication and Tribology*, Vol. 66 No. 4, pp. 509-519.

Safar, Z. and Szeri, A.Z. (1974), "Thermohydrodynamic lubrication in laminar and turbulent regimes", *Journal of Lubrication Technology*, Vol. 96 No. 1, pp. 48-57.

Sharma, N., Kango, S. and Sharma, R.K. (2019), "Adiabatic analysis of microtextured porous journal bearings functioned with power law fluid model", *Proceedings of the Institution of Mechanical Engineers, Part J: Journal of Engineering Tribology*, Vol. 233 No. 10, pp. 1541-1553.

Shin, D., Yang, J., Tong, X., Suh, J. and Palazzolo, A. (2021), "A review of journal bearing thermal effects on rotordynamic response", *Journal of Tribology*, Vol. 143 No. 3, p. 031803.

Simmons, J.E.L. and Dixon, S.J. (1994), "Effect of load direction, preload, clearance ratio, and oil flow on the performance of a 200 mm journal pad bearing", *Tribology Transactions*, Vol. 37 No. 2, pp. 227-236.

Some, S. and Guha, S.K. (2020), "Effect of journal misalignment and coupled-stress lubricant on the film pressure of a double-layered porous journal bearing", *Industrial Lubrication and Tribology*, Vol. 72 No. 3, pp. 315-323.

Sun, J. and Gui, C. (2004), "Hydrodynamic lubrication analysis of journal bearing considering misalignment caused by shaft deformation", *Tribology International*, Vol. 37 No. 10, pp. 841-848.

Sun, J., Zhu, X., Zhang, L., Wang, X., Wang, C., Wang, H. and Zhao, X. (2014), "Effect of surface roughness, viscosity-pressure relationship and elastic deformation on lubrication performance of misaligned journal bearings", *Industrial Lubrication and Tribology*, Vol. 66 No. 3, pp. 337-345.

Tkachuk, M., Shut, O., Marchenko, A., Grabovskiy, A., Lipeiko, A., Polyvianchuk, A. and Igor, G. (2021), "Strength and stability criteria limiting geometrical dimensions of a cantilever impeller", *SAE Technical Paper*, pp. 2021-01-5056.

Visnadi, L.B. and de Castro, H.F. (2019), "Influence of bearing clearance and oil temperature uncertainties on the stability threshold of cylindrical journal bearings", *Mechanism and Machine Theory*, Vol. 134, pp. 57-73.

Wang, L., He, M., Wang, M. and Wei, Y. (2021), "Lubrication performance analysis of multi-groove sleeve bearing considering journal misalignment", *Industrial Lubrication and Tribology*, Vol. 73 No. 4, pp. 588-598.

Xiang, G., Han, Y., Wang, J., Xiao, K. and Li, J. (2019), "A transient hydrodynamic lubrication comparative analysis for misaligned micro-grooved bearing considering axial reciprocating movement of shaft", *Tribology International*, Vol. 132, pp. 11-23.

Xu, G., Zhou, J., Geng, H., Lu, M., Yang, L. and Yu, L. (2015), "Research on the static and dynamic characteristics of misaligned journal bearing considering the turbulent and thermohydrodynamic effects", *Journal of Tribology*, Vol. 137 No. 2, p. 024504.

Yang, T., Han, Y., Wang, Y. and Xiang, G. (2022), "Numerical analysis of the transient wear and lubrication behaviors of misaligned journal bearings caused by linear shaft misalignment", *Journal of Tribology*, Vol. 144 No. 5, p. 051801.

Yang, M., Lu, H., Zhang, X., Zhang, Y.Q., Li, Z.J. and Zhang, W. (2023), "Mixed lubrication performances of misaligned stern bearing considering turbulence and elastic deformation", *Industrial Lubrication and Tribology*, Vol. 75 No. 6, pp. 645-653.

Zhang, J., Yu, F., Zou, D., Ta, N. and Rao, Z. (2019), "Comparison of the characteristics of aerostatic journal bearings considering misalignment under pure-static and hybrid condition", *Proceedings of the Institution of Mechanical Engineers, Part J: Journal of Engineering Tribology*, Vol. 233 No. 5, pp. 769-781.

Zhang, X., Yin, Z., Jiang, D., Gao, G., Wang, Y. and Wang, X. (2016), "Load carrying capacity of misaligned hydrodynamic water-lubricated plain journal bearings with rigid bush materials", *Tribology International*, Vol. 99, pp. 1-13.

Zheng, L., Zhu, H., Fan, S., Wu, J. and Cao, J. (2022), "Theoretical research of couple stress effect and surface roughness on lubrication regimes transition of misaligned hydrodynamic journal", *Proceedings of the Institution of Mechanical Engineers, Part J: Journal of Engineering Tribology*, Vol. 236 No. 12, pp. 2340-2352.

Zhu, S., Sun, J., Li, B. and Zhu, G. (2020), "Thermal turbulent lubrication analysis of rough surface journal bearing with journal misalignment", *Tribology International*, Vol. 144, p. 106109.

About the authors

Xiaodong Sun, a PhD student majoring in Mechanical Engineering from Technical University of Munich. His main research topics include rotor dynamics, hydrodynamic bearing and uncertainty quantification. Xiaodong Sun is the corresponding author and can be contacted at: xiaodong.sun@tum.de

Yuanyuan Liu, a lecturer from Anhui University. His main research topics include acoustic levitation, air film journal bearing and mechanical vibration.

Bettina Chocholaty, a PhD student majoring in Mechanical Engineering from Technical University of Munich. Her main research topics include finite element modeling, sound radiation of floor structures and consideration of jointed structures.

Steffen Marburg, a Professor of Technical University of Munich. The research interests of Steffen Marburg (b. 1965) encompass the development and application of numerical methods for vibroacoustics and aeroacoustics, the experimentally based virtual prototyping of complex models in combination with parameter identification, the consideration and identification of parameter variations and structuralacoustic optimization. Prof. Marburg is Co-Editor-in-Chief of the *Journal of Theoretical and Computational Acoustics* as well as Associate Editor for the *Journal of the Acoustical Society of America* and Editor of the journals *Acoustics Australia and Mechanical Systems and Signal Processing*.